Journal of Dynamical Systems & Geometric Theories
ISSN : 1726-037X (Print) 2169-0057 (Online)
Vol. 22(1 & 2) May & Nov. 2024, pp. 1-34
DOI : 10.47974/JDSGT-2023-001

Dynamics of anisotropic holographic dark energy model with a scalar field and cosmic strings

Y. Aditya †
Department of Mathematics
GMR Institute of Technology
Rajam 532127
Andhra Pradesh
India

U. Y. Divya Prasanthi *
Department of Statistics & Mathematics
College of Horticulture
Dr Y. S. R. Horticultural University
Parvathipuram 535501
Andhra Pradesh
India

Molla Mengesha Nigus §
Department of Mathematics
Debre Berhan University
Debre Berhan
Ethiopia

Abstract

Many academic investigations are now examining dark energy theories in conjunction with cosmic strings and scalar fields since these factors play a crucial part in the examination of the present scenario characterised by the universe's accelerated expansion. A non-static plane-symmetric Tsallis holographic dark energy model is developed in the presence of an attracting massive scalar field and cosmic strings. This paper presents a deterministic solution to the Einstein field equations, using conditions that are both mathematically and theoretically relevant. The model's cosmic dynamical parameters have been determined, including the energy conditions, deceleration parameter (q), statefinders, equation of state parameter (ω_{de}), stability analysis, $r - q$ plane, and $\omega_{de} - \omega'_{de}$ plane. We have also highlighted

† *E-mail:* **aditya.y@gmrit.edu.in**
* *E-mail:* **divyaaug24@gmail.com (Corresponding Author)**
§ *E-mail:* **MollaMengesha@dbu.edu.et**

their physical significance in the description of our model. Given the current observations, observational bounds of cosmological parameters are included. Our dark energy model appears to correspond with recent cosmological findings.

Subject Classification: *83C56, 83F05, 83D05.*

Keywords: *Non-static model, Massive scalar field, Holographic dark energy model, Cosmic strings.*

1. Introduction

Modern cosmological measurements indicate that the expansion of our universe is occurring at an accelerated pace compared to previous eras [1]-[5]. The primary factor contributing to the cosmic acceleration is an enigmatic force referred to as "dark energy (DE)," described by its immense negative pressure. Various studies have been conducted in the academic literature to elucidate the puzzling phenomenon of DE models. Significant dynamical dynamical models include scalar field models [6-7], as well as the holographic DE (HDE) model [8]. Various scholars have examined intriguing evaluations of several DE models and updated theories of gravity [9]-[13]. While analysing dynamical DE models, it is crucial to take into accout the significance of HDE and scalar field (SF). Based on the results obtained from the SF models, it can be shown that SF generates energy in conditions of significant negative pressure, leading to a decrease in the accurate SF potential. In general, there are two distinct categories of scalar meson fields. Zero mass SFs are used to depict long-range interactions, while massive SFs (MSFs) are used to describe short-range interactions.

The evolution of the structures inside the universe is a significant enigma of the current century. After the Big Bang, the early Universe experienced symmetry breakdown, which resulted in the appearance of topological imperfections such as domain walls, cosmic strings, and monopolies. Strings are particularly notable and have immense astronomical importance. The genesis of galaxies is contingent upon the cosmic strings in a crucial manner. The existing findings provide evidence in favour of the hypothesis that the early Universe included an extensive network of strings. Investigating the gravitational impacts of these strings will be intriguing because the gravitational field is generated by cosmic strings in combination with stress energy. Letelier [14]-[15] has prsented the broad relativistic study of strings. Many researchers have investigated the study of cosmic strings, considering several physical origins and various alternative theories of gravity. Literature is abundant with pertinent references on this topic [16-19].

The HDE model has gained popularity in recent years as a dynamic DE model for studying the DE problem. The investigation of quantum gravity has been widely explored in the literature, with a particular focus on the quantum features of black holes (BHs) [20, 21]. Cohen et al. [22] have provided the energy density of HDE as

$$\rho_{de} = 3d^2 m_p^2 L^{-2}. \tag{1}$$

m_p is the Planck mass, $3d^2$ is a constant, and L is the IR cutoff. Several researchers in the literature [23]-[27] have explored several IR-cutoffs. The modified cosmic scenario, as examined by Nojiri et al. [28], is a result of incorporating non-extensive thermodynamics with changing exponents inside a cosmological framework. Nojiri et al. [29] have shown that a diverse range of DE models may be considered distinct contenders within the generalized HDE family, each with its own set of thresholds.

In recent times, a number of entropy formalisms have been used for the purpose of constructing and evaluating cosmological models. The Tsallis HDE (THDE) model, as described in references [30, 31], is a novel HDE model that has not achieved stability at the classical level [30-33]. These efforts are supported by the ability to calculate the Bekenstein entropy by using the Tsallis statistics on the system horizon [34]. The developed models exhibit adequate stability on their own as well [33, 35, 36]. Here are some notable studies on HDE models: Younas et al. [37], Ghaffari et al. [38], Aditya et al. [39], Maity and Debnath [40], Iqbal and Jawad [41], Jawad et al. [42] and Aditya and Prasanthi [43] have investigated the several HDE models in alternative theories of gravity.

Significant theoretical explanations and observable evidence from CMBR support the existence of an anisotropic phase that transforms into an isotropic phase in the universe. Based on these investigations, it appears that the isotropic FRW model might not offer a sufficiently accurate depiction of the constituents that existed in the early universe. The utilization of anisotropic Bianchi models is essential in the description of these noteworthy anomalies. Many researchers have conducted investigations on DE models that incorporate SFs in the context of anisotropic backgrounds, with the explicit intention of accomplishing this objective ([44]-[61]). Aditya et al. [62] examined the DE model in the Lyra manifold when an MSF is present. Aditya and Reddy [63] conducted a study on the DE model in $f(R,T)$ gravity, specifically focusing on the influence of a MSF. The study conducted by Daniel Raju et al. [64]-[66], Aditya et al. [67], Naidu et al. [68, 69], Bhaskara Rao et al. [70, 71] and Aditya et al. [72, 73] have examined many aspects of anisotropic DE models including MSFs and cosmic strings. The dark energy cosmological model with MSFs and cosmic strings offers a rich framework for addressing key questions in cosmology. It not only expands our theoretical understanding of dark energy and cosmic structure formation but also provides testable predictions that can guide observational efforts to explore the universe's fundamental components and evolution.

The present work focuses on the non-static plane-symmetric cosmological model of the universe in Einstein's theory, which includes strings, HDE, and MSF as sources of gravity. Below is an overview of the paper's organisation: Section 2 covers the process of deriving and solving field equations. The dynamical parameters of the constructed model and their physical importance are evaluated in section 3. The concluding section includes final remarks.

2. Field equations and model

The non-static planar symmetric space-time may be represented metrically as follows:

$$ds^2 = e^{2A}\{dt^2 - dr^2 - r^2 d\theta^2 - B^2 dz^2\} \tag{2}$$

where A and B are metric potentials and only functions of time t. Several researchers [74-76] investigated various cosmological models in this background of universe. The field equations proposed by Einstein may be formulated in the context of matter, a DE fluid, and an attracted MSF (here $8\pi G = c = 1$)

$$R_{ij} - \frac{1}{2}Rg_{ij} = -(T_{ij}^{S} + T_{ij}^{de} + T_{ij}^{SF}) \tag{3}$$

$$(T_{ij}^{S} + T_{ij}^{de} + T_{ij}^{SF})_{;j} = 0. \tag{4}$$

T_{ij}^{S}, T_{ij}^{de}, and T_{ij}^{SF} are the stress-energy tensors of cosmic strings, DE fluid, and MSF, respectively. The definitions of the energy-momentum tensors are as follows:

$$T_{ij}^{S} = \rho u_i u_j - \lambda x_i x_j, \quad u_i u^i = 1,\ x^i x_j = -1,\ u^i x_j = 0$$
$$T_{ij}^{de} = (\rho_{de} + p_{de}) u_i u_j - g_{ij} p_{de} \tag{5}$$
$$T_{ij}^{SF} = \phi_{,i}\phi_{,j} - \frac{1}{2}(\phi_{,k}\phi^{,k} - M^2\phi^2)$$

p_{de} & ρ_{de} are the DE fluid's pressure and energy density, ϕ is the MSF, λ is string tension, and M is the SF's mass. The Klein-Gordon equation of the SF is

$$g^{ij}\phi_{;ij} + M^2\phi = 0. \tag{6}$$

The DE fluid's energy-momentum tensor can also be represented as

$$T_{ij}^{de} = diag[\rho_{de}, -p_{de}, -p_{de}, -p_{de}] = diag[1, -\omega_{de}, -\omega_{de}, -\omega_{de}]\rho_{de}. \tag{7}$$

Field Eqs. (3) for the metric (2), using (5)-(7), are

$$e^{-2A}\left[2\ddot{A} + \dot{A}^2 + 2\frac{\dot{A}\dot{B}}{B} + \frac{\ddot{B}}{B}\right] + \frac{\dot{\phi}^2}{2} - \frac{M^2\phi^2}{2} = -\omega_{de}\rho_{de} \tag{8}$$

$$e^{-2A}[2\ddot{A} + \dot{A}^2] + \frac{\dot{\phi}^2}{2} - \frac{M^2\phi^2}{2} = \lambda - \omega_{de}\rho_{de} \tag{9}$$

$$e^{-2A}\left[2\frac{\dot{A}\dot{B}}{B} + 3\dot{A}^2\right] - \frac{\dot{\phi}^2}{2} - \frac{M^2\phi^2}{2} = \rho + \rho_{de} \tag{10}$$

$$\ddot{\phi} + \dot{\phi}\left(\frac{\dot{B}}{B} + 4\dot{A}\right) + M^2\phi = 0 \tag{11}$$

The system of field Eqs. (8)-(12) is made up of four separate equations (because Eq. (12) is a result of field equations (8)-(11)) with A, B, ϕ, ω_{de}, ρ_{de}, ρ, and λ seven unknown parameters. To fully solve the system of field equations, we need three more physically valid conditions that establish a connection between these parameters. Consequently, we are presented with the opportunity to choose among the following physically feasible conditions:

- A relation between metric potential as

$$e^{A} = B^{n} \tag{13}$$

Where n is a constant ([77]-[80]).

- The average scale factor $a(t)$ and the SF ϕ in the model exhibit a power-law relationship [81-82]

$$\phi \propto [a(t)]^k \tag{14}$$

the power index is denoted by k. In the literature, several researchers have looked into different aspects of this relationship ([59]-[71]). Considering the practical implementation of equation (14), we examine the correlation between SF and metric potentials to decrease the complexity of the system

$$\phi = \phi_0\, [a(t)]^k. \tag{15}$$

- The researchers have introduced an original THDE density

$$\rho_{de} = \delta L^{2\gamma-4} \tag{16}$$

where δ is an unknown parameter. We will use the IR cutoff L as the GO scale L_{GO} in this study, which has the following form

$$L_{GO} = (\beta \dot{H}(t) + \alpha H(t)^2)^{\frac{-1}{2}} \tag{17}$$

where α and β are two positive constants. THDE may be written in GO scale by combining (16) and (17)

$$\rho_{de} = \delta(\beta \dot{H}(t) + \alpha H(t)^2)^{-\gamma+2}. \tag{18}$$

Using equations (13) and (15) in Eq. (11), we obtain the metric potentials as follows

$$e^A = \left(\frac{c_1}{k_3} \sinh\left(c_1(k_1+1)t + \frac{c_1 c_2}{k_3} \right) \right)^{\frac{k}{(k_1+1)}}$$

$$B = \left(\frac{c_1}{k_3} \sinh\left(c_1(k_1+1)t + \frac{c_1 c_2}{k_3} \right) \right)^{\frac{1}{(k_1+1)}} \tag{19}$$

and SF ϕ can be obtained as

$$\phi = \phi_0 \left(\frac{c_1}{k_3} \sinh\left(c_1(k_1+1)t + \frac{c_1 c_2}{k_3} \right) \right)^{\frac{n(4k+1)}{3k_1+3}} \tag{20}$$

where $k_1 = \frac{n+4k(n+3)}{3}$, $k_2 = \frac{-3M^2}{n(4k+1)}$, c_1 and c_2 are integrating constants.

The fact that many authors have introduced an average scale factor $a(t) = [sinh(\alpha t)]^{\frac{1}{n}}$ about the analysis of DE models in the anisotropic context, it is noteworthy to state that the solution obtained in this study is both intriguing and logically valid ([83] and [84]). They noted that it produces several potential results that align with existing cosmic observations. Several researchers in the literature have used this particular version of the average scale factor to investigate different aspects of DE theories [85]-[87]. Consequently, exploring the SF model using this hyperbolic solution for average scale factors, as described in Equation (19), is an intriguing opportunity. Using Eq. (19) in Eq. (2) we write our DE model as

$$ds^2 = \left(\frac{c_1}{k_3}\sinh\left(c_1(k_1+1)t + \frac{c_1 c_2}{k_3}\right)\right)^{\frac{2k}{(k_1+1)}} \left\{dt^2 - dr^2 - r^2 d\theta^2 - \left(\frac{c_1}{k_3}\sinh\left(c_1(k_1+1)t + \frac{c_1 c_2}{k_3}\right)\right)^{\frac{2}{(k_1+1)}} dz^2\right\} \quad (21)$$

The metric (21) denotes a DE model with an MSF (20) and cosmic strings. The following dynamical parameters have very much importance in the physical discussion of the model.

3. Cosmological parameters

We will discuss the physical meaning of dynamical parameters in our DE model in the presence of MSFs and cosmic strings in this section.

The model's average scale factor $a(t)$ and volume (V) are calculated as

$$V(t) = [a(t)]^3 = e^{4A}B = \left(\frac{c_1}{k_3}\sinh\left(c_1(k_1+1)t + \frac{c_1 c_2}{k_3}\right)\right)^{\frac{4k+1}{k_1+1}}. \quad (22)$$

Hubble's parameter (H) and expansion scalar (θ) are given by

$$H = 3\theta = \frac{(4k+1)c_1}{3} coth\left(c_1(k_1+1)t + \frac{c_1 c_2}{k_3}\right). \quad (23)$$

From Eqs. (18) and (23), we get the energy density of Tsallis HDE of our model can be obtained as

$$\rho_{de}=\delta\left\{\frac{1}{3}\beta(4k+1)c_1^{\,2}(k_1+1)\left(1-\left(coth\left(c_1(k_1+1)t+\frac{c_1c_2}{k_3}\right)\right)^2\right)\right.$$
$$\left.+\frac{1}{9}\alpha(4k+1)^2c_1^{\,2}\left(coth\left(c_1(k_1+1)t+\frac{c_1c_2}{k_3}\right)\right)^2\right\}^{-\gamma+2}. \quad (24)$$

From Eqs. (9), (19) and (20) we obtain the string tension as

$$\lambda=\left\{-2kc_1^{\,2}(k_1+1)\left(csch\left(c_1(k_1+1)t+\frac{c_1c_2}{k_3}\right)\right)^2\right.$$
$$\left.+k^2c_1^{\,2}\left(coth\left(c_1(k_1+1)t+\frac{c_1c_2}{k_3}\right)\right)^2\right\}\times\left(\frac{c_1}{k_3}\sinh\left(c_1(k_1+1)t+\frac{c_1c_2}{k_3}\right)\right)^{\frac{-2k}{k_1+1}}$$
$$-\left\{-2kc_1^{\,2}(k_1+1)\left(csch\left(c_1(k_1+1)t+\frac{c_1c_2}{k_3}\right)\right)^2\right.$$
$$\times\left(\frac{c_1}{k_3}\sinh\left(c_1(k_1+1)t+\frac{c_1c_2}{k_3}\right)\right)^{\frac{-1}{(k_1+1)}}+c_1^{\,2}\left(1-k_1\left(csch\left(c_1(k_1+1)t+\frac{c_1c_2}{k_3}\right)\right)^2\right)$$
$$\left.\times\left(\frac{c_1}{k_3}\sinh\left(c_1(k_1+1)t+\frac{c_1c_2}{k_3}\right)\right)^{-(k_1+1)^{-1}}\right\}\times\left(\frac{c_1}{k_3}\sinh\left(c_1(k_1+1)t+\frac{c_1c_2}{k_3}\right)\right)^{\frac{-2k}{k_1+1}} \quad (25)$$

From equations (10), (19), (20) and (25), we get the tension density as

$$\rho=\left\{2kc_1^{\,2}\left(coth\left(c_1(k_1+1)t+\frac{c_1c_2}{k_3}\right)\right)^2\left(\frac{c_1}{k_3}\sinh\left(c_1(k_1+1)t+\frac{c_1c_2}{k_3}\right)\right)^{\frac{-1}{(k_1+1)}}\right.$$
$$\left.+3k^2c_1^{\,2}\left(coth\left(c_1(k_1+1)t+\frac{c_1c_2}{k_3}\right)\right)^2\right\}\left(\frac{c_1}{k_3}\sinh\left(c_1(k_1+1)t+\frac{c_1c_2}{k_3}\right)\right)^{\frac{-2k}{k_1+1}}$$
$$-\frac{M^2\phi_0^{\,2}}{2}\left(\frac{c_1}{k_3}\sinh\left(c_1(k_1+1)t+\frac{c_1c_2}{k_3}\right)\right)^{\frac{2n(4k+1)}{3k_1+3}}-\frac{1}{18}\phi_0^{\,2}n^2c_1^{\,2}$$
$$(4k+1)^2\left(\frac{c_1}{k_3}\sinh\left(c_1(k_1+1)t+\frac{c_1c_2}{k_3}\right)\right)^{\frac{2n(4k+1)}{3k_1+3}}\left(coth\left(c_1(k_1+1)t+\frac{c_1c_2}{k_3}\right)\right)^2-\rho_{de}.$$
$$(26)$$

Scalar field:

Fig. 1 illustrates the relationship between a SF (Eq. (20)) and time for different values of n. For all values of n, the SF exhibits a decreasing pattern throughout cosmic time, as seen in Fig. 1. It is seen that the SF is decreasing, leading to an increase in kinetic energy. The observed behaviour bears a resemblance to the SF behaviour seen in DE SF models developed by many authors (Ref. [64-66] and [88]). The SF diminishes as the value of n increases. To examine the impact of the SF on the development of other cosmological parameters, we studied the other dynamical parameters for different values of n.

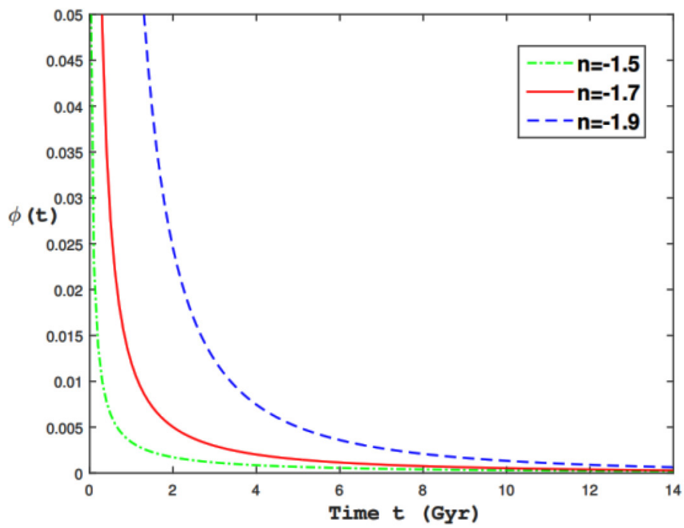

Figure 1

Scalar field Vs. t **for** $k = 0.5,\ c_1 = 0.075,\ c_2 = 0.025,\ M = 0.45$ **and** $\phi_0 = 0.0001$.

String tension:

The equation of state (EoS) of cosmic strings is restricted by the energy conditions. With $\rho > 0$ or $\lambda < 0$, the weak and strong energy conditions result in $\rho \geq \lambda$. The domestic energy conditions imply $\rho \geq 0$ and $\rho^2 \geq \lambda^2$. The signature of λ is not constrained by these energy conditions. We have plotted the behaviour of string tension λ in terms of time t for different values of other model parameters in Fig. 2. It can be seen from Fig. 2 that the string tension is negative throughout the evolution of the universe and finally vanishes.

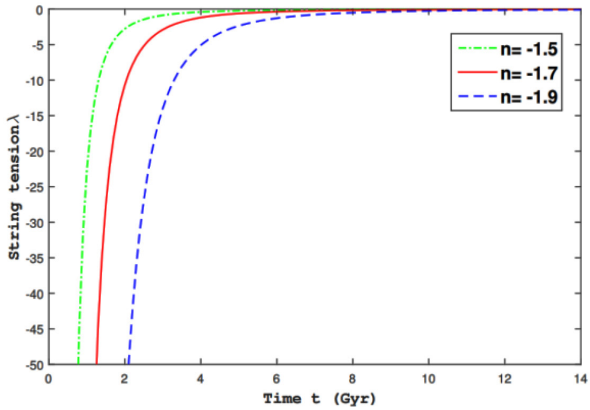

Figure 2

String tension λ **Vs.** t **for** $k = 0.5$, $c_1 = 0.075$, $c_2 = 0.025$ **and** $M = 0.45$.

Energy conditions:

The Null energy conditions (NEC) $(\rho_{eff} + p_{de} \geq 0)$ suggests that the universe's energy density drops as it expands, and its violation may result in the Big Rip of cosmology. The accelerating expansion of the universe is represented by the violation of the strong energy conditions (SEC) $(\rho_{eff} + 3p_{de} \geq 0,\ \rho_{eff} + p_{de} \geq 0)$ conditions. The validity of SEC $(\rho_{eff} + 3p_{de} \geq 0,$

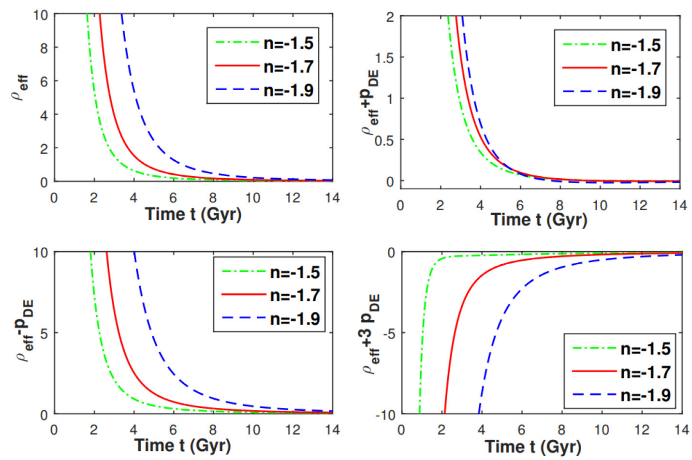

Figure 3

Energy conditions Vs. t **for** $k = 0.5$, $c_1 = 0.075$, $c_2 = 0.025$, $M = 0.45$, $\phi_0 = 0.0001$, $\alpha = 0.8502$, $\beta = 0.4817$, $\gamma = 1.22$, **and** $\delta = 2.5$.

$\rho_{eff} + p_{de} \geq 0)$ and weak energy conditions (WEC) $(\rho_{eff} + p_{de} \geq 0,\ \rho_{eff} \geq 0)$ are indicated by the Hawking-Penrose singularity theorems. The WEC and NEC are essential among all the other energy conditions because their failure causes other energy conditions to be violated.

Fig. 3 displays the energy conditions for various values of in our model. The NEC is first fulfilled and then violated. Consequently, the model generates a significant impact. Furthermore, our approach must comply with the SEC. It is important to mention that the WEC is satisfied, but the dominant energy condition (DEC) $(\rho_{eff} \pm p_{de} \geq 0,\ \rho_{eff} \geq 0)$ is not. The observed orientation may be attributed to the late-time acceleration of the universe, a phenomenon that aligns with existing data from experiments.

Deceleration parameter:

The deceleration parameter (DP) is used in the computation of the rate at which the universe expands. The term is defined as:

$$q = -1 - \frac{\dot{H}}{H^2}. \tag{27}$$

The nature of the universe's expansion is explained using DP's signature. The deceleration phase is shown by positive values of DP, whereas the model exhibits accelerated expansion for $-1 \leq q < 0.$ The DP is calculated as follows in our model:

$$q = -1 + \frac{3k_1 + 3}{4k + 1}\left(sech\left(c_1(k_1 + 1)t + \frac{c_1 c_2}{k_3} \right) \right)^2. \tag{28}$$

The behavior of DP for our constructed model with respect to time is seen in Fig. 4. Our model exhibits a distinct shift from positive to negative values, indicating a smooth transition from the initial period of deceleration to the present age of acceleration in the universe. The acceleration of expansion in our model starts at a point $t_s \approx 6.2\,Gyr$ i.e., 7.5 Gyr ago from the present $(t_0 = 13.7\,Gyr),$ resulting in a current value of DP of $q = -0.75.$ The behaviour of the DP is supported by data obtained from several observational approaches ([89]-[92]).

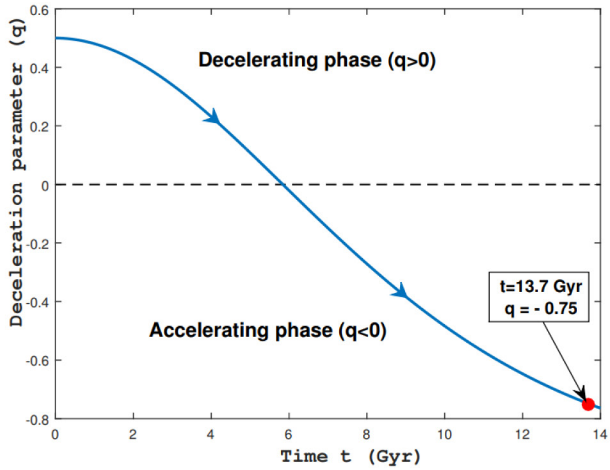

Figure 4

DP Vs. t **for** $k=0.5,\ c_1=0.075,\ c_2=0.025,\ M=0.45,\ \phi_0=0.0001,$ $\alpha=0.8502,\ \beta=0.4817,\ \gamma=1.22,$ **and** $\delta=2.5.$

EoS parameter:

The EoS parameter (ω_{de}) of our model is constructed as

$$
\begin{aligned}
\omega_{de}=&\left\{\left\{2kc_1^{\,2}(k_1+1)\left(csch\left(c_1(k_1+1)t-\frac{c_1c_2}{k_3}\right)\right)^2+k^2c_1^{\,2}\left(coth\left(c_1(k_1+1)t+\frac{c_1c_2}{k_3}\right)\right)^2\right.\right.\\
&\left.-2kc_1^{\,2}\left(coth\left(c_1(k_1+1)t+\frac{c_1c_2}{k_3}\right)\right)^2\right\}\left(\left(\frac{c_1}{k_3}\sinh\left(c_1(k_1+1)t+\frac{c_1c_2}{k_3}\right)\right)^{-(k_1+1)^{-1}}\right)\\
&\left.-c_1^{\,2}\left(1-k_1\left(csch\left(c_1(k_1+1)t+\frac{c_1c_2}{k_3}\right)\right)^2\right)\left(\frac{c_1}{k_3}\sinh\left(c_1(k_1+1)t+\frac{c_1c_2}{k_3}\right)\right)^{\frac{-1}{(k_1+1)}}\right\}\\
&\times\left(\frac{c_1}{k_3}\sinh\left(c_1(k_1+1)t+\frac{c_1c_2}{k_3}\right)\right)^{\frac{-2k}{k_1+1}}+\frac{M^2\phi_0^{\,2}}{2}\left(\frac{c_1}{k_3}\sinh\left(c_1(k_1+1)t+\frac{c_1c_2}{k_3}\right)\right)^{\frac{2n(4k+1)}{3k_1+3}}\\
&-\frac{\phi_0^{\,2}n^2c_1^{\,2}(4k+1)^2}{18}\left(\frac{c_1}{k_3}\sinh\left(c_1(k_1+1)t+\frac{c_1c_2}{k_3}\right)\right)^{\frac{2n(4k+1)}{3k_1+3}}
\end{aligned}
$$

$$\times\left[\left(coth\left(c_1(k_1+1)t+\frac{c_1c_2}{k_3}\right)\right)^2\times\delta\left\{\left(1-\left(coth\left(c_1(k_1+1)t+\frac{c_1c_2}{k_3}\right)\right)^2\right)\right.\right.$$
$$\left.\times\frac{\beta}{3}(4k+1)c_1^{\;2}(k_1+1)+\frac{\alpha}{9}(4k+1)^2c_1^{\;2}\left(coth\left(c_1(k_1+1)t+\frac{c_1c_2}{k_3}\right)\right)^2\right\}^{-\gamma+2} \tag{29}$$

Fig. 5 illustrates the relationship between our model and time for several values of n. The evolution of the EoS parameter is evident as it transitions from an era of aggressive phantom $(\omega_{de} << -1)$ to the phase of phantom dominance $(\omega_{de} < -1)$ in the universe. When the magnitude of the SF $\phi(t)$ increases, the EoS parameter in our proposed model tends to approach the aggressive phantom region. The current values of the EoS parameters (n,ω_{de}) = $(-1.5,\ -0.64)$, (n,ω_{de}) = $(-1.7,\ -1.045)$, and (n,ω_{de}) = $(-1.9,\ -2.192)$ are consistent with modern observational data reported by Aghanim et al. [93].

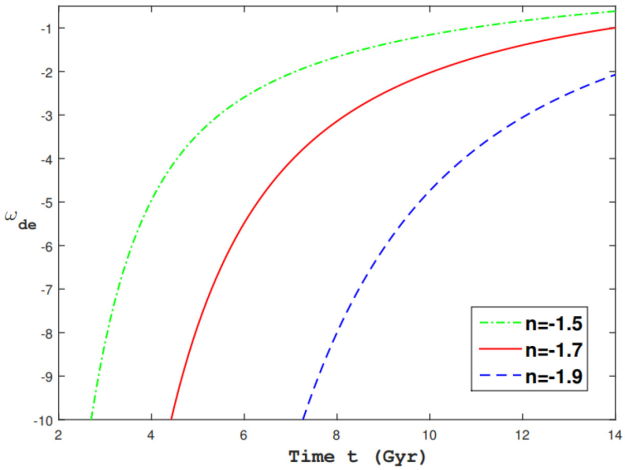

Figure 5

Plot of EoS parameter versus cosmic time t **for** $k=0.5,\ c_1=0.075,\ c_2=0.025,\ M=0.45,\ \phi_0=0.0001,\ \alpha=0.8502,\ \beta=0.4817,\ \gamma=1.22,$ **and** $\delta=2.5.$

Squared sound speed:

The squared sound speed (v_s^2) parameter is used to assess the stability of DE models, with stability being influenced by its sign. The stability of our proposed model is determined by the positive sign of v_s^2, whereas the model's instability is determined by the negative sign of v_s^2. This is how it is defined:

$$v_s^2 = \frac{\dot{p}_{de}}{\dot{\rho}_{de}} = \omega_{de} + \frac{\rho_{de}}{\dot{\rho}_{de}}\dot{\omega}_{de}. \tag{30}$$

v_s^2 may be determined by substituting formulae for the parameters in Equation (30). As seen in Fig. 6, we conducted a quantitative analysis of the squared sound speed v_s^2 by plotting it against time. The consistent negative nature of throughout the universe's history implies the model's fundamental instability. This inclination aligns with the recent findings in observational data.

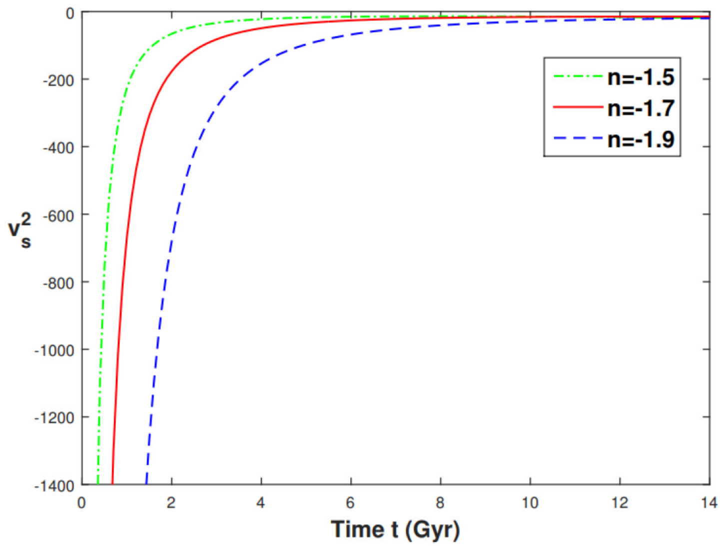

Figure 6

v_s^2 **Vs.** t **for** $k = 0.5$, $c_1 = 0.075$, $c_2 = 0.025$, $M = 0.45$, $\phi_0 = 0.0001$, $\alpha = 0.8502$, $\beta = 0.4817$, $\gamma = 1.22$, **and** $\delta = 2.5$.

$\omega_{de} - \omega'_{de}$ plane:

$\omega_{de} - \omega'_{de}$ plane is divided into two regions: freezing $(\omega'_{de} < 0,\ \omega_{de} < 0)$ and thawing $(\omega'_{de} > 0,\ \omega_{de} < 0)$ (Caldwell and Linder [94]). Fig. 7 depicts the variation of the $\omega_{de} - \omega'_{de}$ plane for our constructed cosmological model. The $\omega_{de} - \omega'_{de}$ plane has been shown to represent a thawing zone in the evolution of the universe.

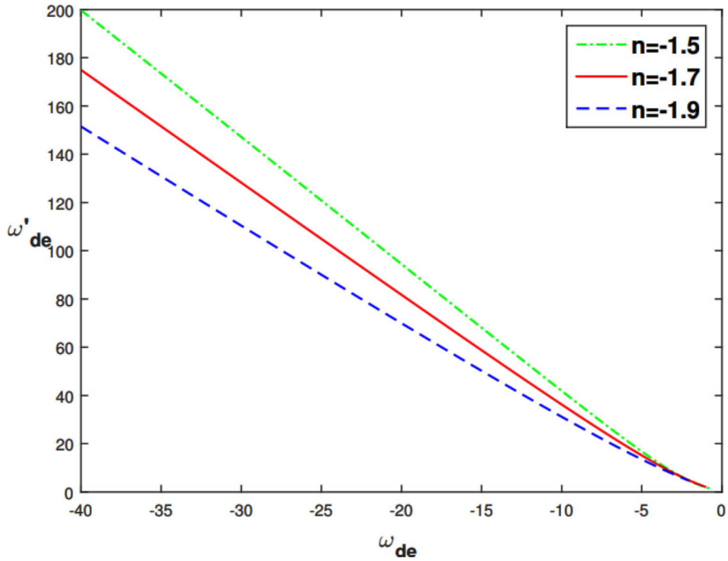

Figure 7

$\omega_{de} - \omega'_{de}$ **plane for** $k = 0.5,\ c_1 = 0.075,\ c_2 = 0.025,\ M = 0.45,\ \phi_0 = 0.0001,$ $\alpha = 0.8502,\ \beta = 0.4817,\ \gamma = 1.22,$ **and** $\delta = 2.5.$

Statefinder parameters:

Sahni et al. [95] proposed statefinders as follows:

$$r = \frac{\dddot{a}}{aH^3},\quad s = \frac{r-1}{3\left(q - \frac{1}{2}\right)} \tag{31}$$

The regions are defined as follows by these statefinders: cosmological models for $(r,s) = (1,0)$ and $(r,s) = (1,1)$ are ΛCDM and CDM, respectively. The quintessence and phantom DE phases are produced by the $r < 1$ and $s > 0$ regions. $r > 1$ and $s < 0$ represents the Chaplygin gas model. The behaviour of $r - s$ plane for our constrcuted model is shown in Fig. 8. The statefinder plane's trajectory may be shown to eventually meet the ΛCDM limit. In the $r - s$ trajectory, the phantom and quintessence properties can also be seen.

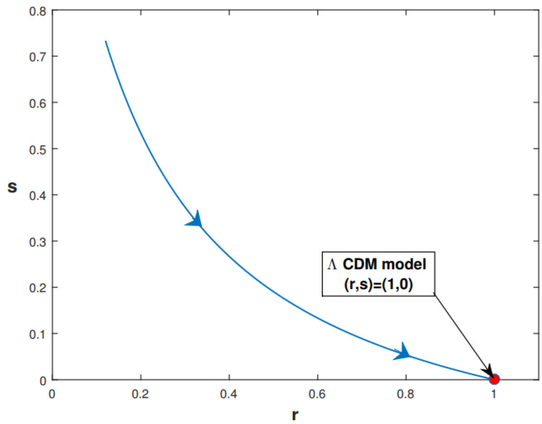

Figure 8

$r-s$ **plane for** $k=0.5,\ c_1=0.075,\ c_2=0.025,\ M=0.45,\ \phi_0=0.0001,\ \alpha=0.8502,\ \beta=0.4817,\ \gamma=1.22,$ **and** $\delta=2.5.$

$r-q$ plane:

The evolution of our constructed model in the plane is seen in Fig. 9. We start our model with the SCDM model and then transition to the SS model. It is evident from the $r-q$ trajectory that our model has similarities to the quintessence SF model proposed by several authors in the leterature ([50], [96]).

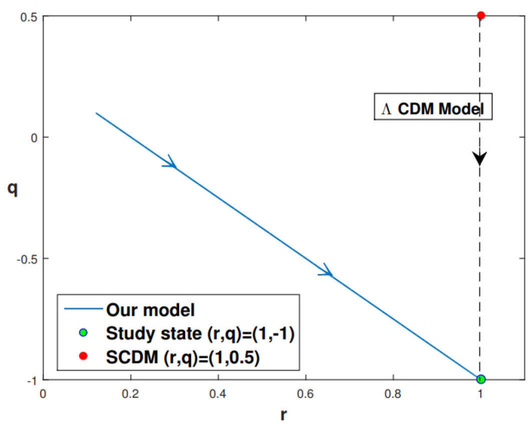

Figure 9

$r-q$ **plane for** $k=0.5,\ c_1=0.075,\ c_2=0.025,\ M=0.45,\ \phi_0=0.0001,\ \alpha=0.8502,\ \beta=0.4817,\ \gamma=1.22,$ **and** $\delta=2.5.$

Observational bounds:

Here, we would like to discuss observational bounds on the important parameters like k, n and γ. For this purpose, we consider Planck collaboration data as a whole (Aghanim et al. [93]) for the EoS parameter:

$$\omega_{de}\begin{cases} -1.56^{+0.60}_{-0.48}\,(\text{Planck}+\text{lowE}+\text{TT}) \\ -1.58^{+0.52}_{-0.41}\,(\text{Planck}+\text{lowE}+\text{TT},\text{TE},\text{EE}) \\ -1.57^{+0.50}_{-0.40}\,(\text{Planck}+\text{lensing}+\text{TT},\text{TE},\text{EE}+\text{lowE}) \\ -1.04^{+0.10}_{-0.10}\,(\text{Planck}+\text{lensing}+\text{BAO}+\text{TT},\text{TE},\text{EE}+\text{lowE}). \end{cases}$$

It can be observed from tables-1(a) to 1(c) that we fit the parameters k, n and γ to satisfy the current value of the EoS parameter given by Planck + lowE+ TT observations. Similarly, in tables-2(a) to 2(f) we have obtained the observational bounds on k, n and γ given the present values of EoS parameter given by Planck +lensing+TT, TE, EE+lowE and Planck +lensing+BAO+ TT, TE, EE+lowE. For $\gamma = 1$, our Tsallis HDE model becomes an ordinary HDE model. Hence we have chosen $\gamma = 1$ as a special case to estimate the observational bounds in each table.

The current value of the deceleration parameter from numerous observations (Caunha [89]; Li et al. [90]; Amirhashchi and Amirhashchi [91]; Capozziello et al. [92]) is given by

$$q = -0.930 \pm 0.218\ (\text{BAO+ TDSL+ Masers+ Pantheon}\,H_2)$$
$$q = -1.2037 \pm 0.175\ (\text{BAO} + \text{TDSL} + \text{Masers} + \text{Pantheon} + H_2 + \text{H}_0).$$

In table-3, we fit the parameters k and n to satisfy the current value of the deceleration parameter given the above-mentioned observational data.

In tables-4(a) to 4(c), we obtain the observational bounds on the parameters n and k to discuss the nature of our model using statefinders. It can be seen from the table that we can choose the values of n and k for different epochs of the universe (quintessence, phantom and Chaplygin).

According to tables-1(a) to 4(c), some parameter combinations will result in the correct EoS parameter (W_{de}) or deceleration parameter (q) or statefinder parameters (r, s), one at a time. However, we made an effort to show that there are model parameter combinations that are simultaneously consistent with all observational constraints to establish the viability of our model. From tables-5(a) and 5(b) we obtain model parameters that are simultaneously consistent with all observational constraints.

Table 1(a)

Table represents the EoS parameter at the present epoch for different values of parameters k, n and $\gamma = 0$.

$\gamma = 0$			
k	n	ω_{de}	Planck + lowE+ TT
.42	-1.08	-1.997	$-1.56^{+0.60}_{-0.48}$
.46	-1.04	-1.685	
.5	-1	-1.428	
.54	-0.96	-1.215	
.6	-0.9	-0.96	

Table 1(b)

Table represents the EoS parameter at the present epoch for different values of parameters k, n and γ.

k	n	γ	ω_{de}	Planck + lowE+ TT
.8875	-1.79	0.71	-1.9	$-1.56^{+0.60}_{-0.48}$
.925	-1.76	0.74	-1.325	
.9375	-1.75	0.75	-1.179	
.95	-1.74	0.76	-1.051	
.5375	-2.07	1.43	-1.477	
.5625	-2.05	1.45	-0.965	

Table 1(c)

Table represents the EoS parameter at the present epoch for different values of parameters k, n and $\gamma = 1$.

$\gamma = 1$			
k	n	ω_{de}	Planck + lowE+ TT
.65	-1.85	-1.966	$-1.56^{+0.60}_{-0.48}$
.69	-1.81	-1.387	
.71	-1.79	-1.181	
.73	-1.77	-1.014	

Table 2(a)

Table represents the EoS parameter at the present epoch for different values of parameters k, n and $\gamma = 0$.

$\gamma = 0$			
k	n	ω_{de}	Planck +lowE+ TT, TE, EE & Planck +lensing+TT, TE, EE+lowE
.4625	-1.33	-1.899	$-1.58^{+0.52}_{-0.41}$ & $-1.57^{+0.50}_{-0.40}$
.5	-1.3	-1.612	
.5125	-1.29	-1.528	
.525	-1.28	-1.448	
.55	-1.26	-1.303	
.5625	-1.25	-1.237	
.5875	-1.23	-1.115	

Table 2(b)

Table represents the EoS parameter at the present epoch for different values of parameters k and n.

$\gamma = 1$			
k	n	ω_{de}	Planck +lowE+ TT, TE, EE & Planck +lensing+TT, TE, EE+lowE
.7125	-1.93	-1.79	$-1.58^{+0.52}_{-0.41}$ & $-1.57^{+0.50}_{-0.40}$
.725	-1.92	-1.609	
.7375	-1.91	-1.451	
.75	-1.9	-1.313	
.7625	-1.89	-1.192	
.775	-1.88	-1.085	

Table 2(c)

Table represents the EoS parameter at the present epoch for different values of parameters k, n and γ.

k	n	γ	ω_{de}	Planck +lowE+ TT, TE, EE & Planck +lensing+TT, TE, EE+lowE
.8875	-1.79	0.71	-1.9	$-1.58^{+0.52}_{-0.41}$ & $-1.57^{+0.50}_{-0.40}$
.925	-1.76	0.74	-1.325	
.9375	-1.75	0.75	-1.179	
.525	-2.08	1.42	-1.846	
.5375	-2.07	1.43	-1.477	

Table 2(d)

Table represents the EoS parameter at the present epoch for different values of parameters k and n.

$\gamma = 0$			
k	n	ω_{de}	Planck + lensing + BAO + TT, TE, EE+lowE
.5875	-1.23	-1.115	$-1.04^{+0.10}_{-0.10}$
.6	-1.22	-1.059	
.6125	-1.21	-1.007	
.625	-1.2	-0.957	

Table 2(e)

Table represents the EoS parameter at the present epoch for different values of parameters k and n.

$\gamma = 1$			
k	n	ω_{de}	Planck + lensing + BAO + TT, TE, EE+lowE
.775	-1.88	-1.085	$-1.04^{+0.10}_{-0.10}$
.7875	-1.87	-0.99	

Table 2(f)

Table represents the EoS parameter at the present epoch for different values of parameters k, n and γ.

k	n	γ	ω_{de}	Planck + lensing + BAO + TT, TE, EE+lowE
.9317	-1.73	0.77	-1.068	$-1.04^{+0.10}_{-0.10}$
.9438	-1.72	0.78	-0.954	
.5625	-2.05	1.45	-0.965	

Table 3

The table represents the deceleration parameter at the present epoch for different values of parameters *k* and *n*.

n	k	q	BAO + TDSL + Masers + Pantheon H_z & BAO + TDSL +Masers + Pantheon + H_z + H_0
-0.7	0.3	-0.73	-0.930 ± 0.218 & -1.2037 ± 0.175
-0.2	0.4	-0.92	
-1.6	0.5	-0.72	
-1.8	0.6	-0.74	
-1.7	0.6	-0.77	
-0.7	0.6	-0.96	
-1.8	0.7	-0.81	
-1.8	0.8	-0.86	
-1.8	0.9	-0.9	

Table 4(a)

The table represents the statefinder parameters limits (Phantom model) for different values of parameters *k* and *n*.

Phantom model $s > 0$		
N	k	s
-0.7	0.3	0.198
-0.1	0.4	0.05
-1.8	0.6	0.056
-0.9	0.7	0.001
-0.1	0.7	0.003
-2	0.8	0.001
-1.9	0.9	0.024
-1.9	1.1	0.001

Table 4(b)

The table represents the statefinder parameters limits (Chapygin gas model) for different values of parameters *k* and *n*.

Chaplygin gas model $r > 1$ and $s < 0$			
n	K	r	s
-0.5	0.3	1.492	-0.109
-1.1	0.4	3.086	-0.464
-1.4	0.5	2.043	-0.232
-1.5	0.6	1.806	-0.179

Contd...

-0.9	0.8	1.107	-0.024
-1.2	0.9	1.042	-0.009
-1.4	1.1	1.009	-0.002
-1.3	1.4	1	0

Table 4(c)

The table represents the statefinder parameters limits for different values of parameters k and n.

Quintessence model $r < 1$		
n	k	r
-1.1	0.4	0.64
-1.5	0.5	0.51
-0.1	0.5	0.961
-0.8	0.6	0.845
-1.9	0.7	0.991
-1.9	0.9	0.893
-1.2	1.1	0.968
-0.5	1.1	0.994

Table 5(a)

The table represents the deceleration parameter, EoS parameter and statefinder parameters limits for different values of parameters γ, k and n.

Quintessence model $r < 1$				
n	k	Q	w_{de}	γ
-1.58	1.68	-0.997	-0.979	0
-1.61	1.5	-0.994	-0.975	0.2
-1.52	1.17	-0.982	-0.986	0.5
-1.58	1.08	-0.969	-0.985	0.6
-1.55	0.75	-0.897	-0.982	0.9
-1.58	0.66	-0.847	-0.975	1
-1.73	0.54	-0.717	-0.978	1.2

Table 5(b)

The table represents the deceleration parameter, EoS parameter and statefinder parameters limits for different values of parameters γ, k and n.

Phantom model $s > 0$				
n	**k**	**q**	w_{de}	γ
-1.97	1.8	-0.988	-1.006	0
-1.97	1.62	-0.98	-1.012	0.2
-1.55	1.38	-0.992	-1	0.3
-2	1.44	-0.963	-1.048	0.4
-1.97	1.23	-0.941	-1.038	0.6
-2	1.05	-0.895	-1.047	0.8
-1.7	0.69	-0.832	-1.059	1

4. Results and Conclusions

A wide range of researchers worldwide are attracted by the concept of the universe's accelerated expansion. Various methodologies have been suggested to investigate this possibility, including alternate theories of gravity and other dynamical DE models. The present research focuses on the investigation of a non-static plane-symmetric THDE cosmological model within the framework of the general theory of gravity. This model incorporates an attracting MSF and cosmic strings. Prominent cosmic parameters and planes have been determined.

Early inflation occurs due to the expansion of the model from a finite volume. The model exhibits finite physical quantities at $t \to \infty$ and infinite physical quantities at $t = 0$. Consequently, our model exhibits an initial singularity, meaning that our representation of the universe starts with a big bang and thereafter expands exponentially. The model exhibits homogeneity and uniformity throughout its whole and then attains isotropy and shear-free behaviour near the end. The SF reduces as cosmic time increases for all parameter values n, and it also decreases as n increases. It is seen that the SF is undergoing a decrease, leading to an increase in kinetic energy. The observed behaviour has a resemblance to the SF models of DE that have been developed by many authors (references [88] and [64-66]). The NEC are satisfied at the initial epoch and violated at later times. As a result, the model creates a Big Rip. It is also noting that the WEC is satisfied, however, the DEC is not. This tendency is due to the universe's accelerated expansion, which is consistent with modern observational evidence. The study of the DP reveals that our constructed model exhibits a transition from the early deceleration era to the current acceleration epoch. It can also be seen that our DE model entered into accelerating expansion at $t_s \approx 6.2\,Gyr$, i.e. 7.5 Gyr ago from today (t = 13.7 Gyr) and the current value of the DP may be found to be -0.75. This is consistent with data from many schemes

$$q = -0.930 \pm 0.218 \text{ (BAO + TDSL + Masers + Pantheon } H_z\text{)}$$
$$q = -1.2037 \pm 0.175 \text{(BAO + TDSL + Masers + Pantheon} + H_z + H_0\text{) ([89] - [92]).}$$

Our THDE model evolves from the aggressive phantom era $(\omega_{de} << -1)$ to the phantom-dominated phase $(\omega_{de} < -1)$ of the universe. When the SF $\phi(t)$ grows, our THDE model approaches the aggressive phantom region. The current values of the EoS parameter (n, ω_{de}) = (–1.5, –0.64), (n, ω_{de}) = (–1.7, –1.045), and (n, ω_{de}) = (–1.9, –2.192) are all in good accordance with recent observational data. The following is a list of the Planck collaboration data as a whole (Aghanim et al. [93]):

$$\omega_{de} = \begin{cases} -1.56^{+0.60}_{-0.48} \text{ (Planck + lowE + TT)} \\ -1.58^{+0.52}_{-0.41} \text{ (Planck + lowE + TT, TE, EE)} \\ -1.57^{+0.50}_{-0.40} \text{ (Planck + lensing + TT, TE, EE + lowE)} \\ -1.04^{+0.10}_{-0.10} \text{ (Planck + lesing + BAO + TT, TE, EE + lowE)} \end{cases}$$

Throughout the evolution of the universe, the $\omega_{de} - \omega'_{de}$ plane has been observed to represent a thawing zone. Squared sound speed v_s^2 is negative throughout the universe's evolution indicating that the model is unstable. This behaviour is consistent with what has been reported recently. It can be shown that the statefinder plane's trajectory eventually reaches the ΛCDM limit. The phantom and quintessence characteristics can also be seen in the $r - s$ trajectory. Given the present observational data from various schemes we have added observational bounds to the important parameters like *k*, *n* and γ. For this purpose, we fit the parameters *k*, *n* and γ to satisfy the present values of EoS and deceleration parameters from current observations (Ref. tables-1(a) to 5(b)).

Finally, here is a brief overview of our findings:

- According to recent data, the DP reveals a transition from the early decelerated phase to the current cosmic acceleration.
- When compared to current measurements, the EoS parameter has phantom behaviour and consistent ranges.
- $\omega_{de} - \omega'_{de}$ plane shows a thawing region.

- Our constructed model has been unstable.
- The NEC are satisfied at the initial era and violated at later times. The WEC are satisfied, however, the DEC are not. This is consistent with current observational evidence.
- $r-q$ plane exhibits that our model starts with the SCDM model and then moves on to the steady state model.
- The statefinder parameters correspond to the ΛCDM limit, as well as quintessence and phantom behaviour.

In summary, analysis of the THDE model with MSFs is effective in representing the universe's evolution, from early decelerated phase to late-time acceleration. It would be interesting to undertake more investigations on the generalized HDE models ([29]) and the well-known phenomenon known as holographic inflation (Nojiri et al. [97]; Elizalde and Timoshkin [98]; Nojiri et al. [99]). To extract the overall characteristics of the models, it would also be intriguing to incorporate a joint observational study using information from numerous observations. These essential studies are outside the focus of this work and are reserved for future works.

References

[1] A. G. Riess, A. V. Filippenko, P. Challis, A. Clocchiatti, A. Diercks, P. M. Garnavich, R. L. Gilliland, C. J. Hogan, S. Jha, R. P. Kirshner, B. Leibundgut, M. M. Phillips, D. Reiss, B. P. Schmidt, R. A. Schommer, R. Chris Smith, J. Spyromilio, Ch. Stubbs, N. B. Suntzeff, and J. Tonry, "Observational Evidence from Supernovae for an Accelerating Universe and a Cosmological Constant," *Astronomical Journal*, vol. 116, pp. 1009–1038 (1998).

[2] S. Perlmutter, G. Aldering, G. Goldhaber, R. A. Knop, P. Nugent, P. G. Castro, S. Deustua, S. Fabbro, A. Goobar, D. E. Groom, I. M. Hook, A. G. Kim, M. Y. Kim, J. C. Lee, N. J. Nunes, R. Pain, C. R. Pennypacker, R. Quimby, C. Lidman, R. S. Ellis, M. Irwin, R. G. McMahon, P. Ruiz-Lapuente, N. Walton, B. Schaefer, B. J. Boyle, A. V. Filippenko, T. Matheson, A. S. Fruchter, N. Panagia, H. J. M. Newberg, W. J. Couch, "Measurements of Ω and Λ from 42 High-Redshift Supernovae," *Astrophys. J.*, vol. 517, pp. 565 (1999).

[3] R. R. Caldwell and M. Doran, “Cosmic microwave background and supernova constraints on quintessence: Concordance regions and target models,” *Phys. Rev. D*, vol. 69, pp. 103517 (2004).

[4] S. F. Daniel, “Large scale structure as a probe of gravitational slip,” *Phys. Rev. D*, vol. 77, pp. 103513 (2008).

[5] H. Hoekstra and B. Jain, “Weak Gravitational Lensing and Its Cosmological Applications,” *Annu. Rev. Nucl. Part. Sci.*, vol. 58, pp. 99 (2008).

[6] B. Ratra and J. Peebles, “Cosmological consequences of a rolling homogeneous scalar field,” *Phys. Rev. D*, vol. 37, pp. 321 (1988).

[7] T. Chiba, T. Okabe, and M. Yamaguchi “Kinetically driven quintessence,” *Phys. Rev. D*, vol. 62, pp. 023511 (2000).

[8] A. G. Cohen1, D. B. Kaplan, and A. E. Nelson, “Effective Field Theory, Black Holes, and the Cosmological Constant,” *Phys. Rev. Lett.*, vol. 82, pp. 4971 (1999).

[9] E. J. COPELAND, M. SAMI, and S. TSUJIKAWA, “Dynamics of dark energy,” *Int. J. Mod. Phys. D*, vol. 15, pp. 1753 (2006).

[10] K. Bamba, S. Capozziello, S. Nojiri, S. D. Odintsov “Dark energy cosmology the equivalent description via different theoretical models and cosmography tests,” *Astrophys. Space Sci.*, vol. 342, pp. 155 (2012).

[11] S. Nojiri and S. D. Odintsov, “Unified cosmic history in modified gravity: from F(R) theory to Lorentz non-invariant models,” *Phys. Rept.*, vol. 505, pp. 59 (2011).

[12] T. Harko and F. S. N. Lobo, “Generalized Dark Gravity,” *Int. J. Mod. Phys. D*, vol. 21, pp. 1242019 (2012).

[13] S. Nojiri and S. D. Odintsov, “Introduction to Modified Gravity and Gravitational Alternative for Dark Energy,” *Int. J. Geom. Meth. Mod. Phys.*, vol. 4, pp. 115 (2007).

[14] P. S. Letelier, “Clouds of strings in general relativity,” Phys. Rev. D, vol. 20, pp. 1294 (1979).

[15] P. S. Letelier, “String cosmologies,” *Phys. Rev. D*, vol. 28, pp. 2414 (1983).

[16] K. D. Naidu, Y. Aditya, D.R.K. Reddy, “Cosmic strings in a five dimensional spherically symmetric background in f(R,T) gravity,” *Astrophys. Space Sci.*, vol. 363, pp. 158 (2018).

[17] S. H. Shekh and V. R. Chirde, "Accelerating Bianchi type dark energy cosmological model with cosmic string in f(T) gravity," *Astrophys. Space Sci.*, vol. 365, pp. 60 (2020).

[18] Y. Aditya and D. R. K. Reddy, "Locally rotationally symmetric Bianchi type-I string cosmological models in f(R) theory of gravity," *Int. J. Geom. Theories Mod. Phys.*, vol. 15, pp. 1850156 (2020).

[19] P. K. Sahoo, P. Sahoo, and B. K. Bishi., "Mixed fluid cosmological model in f(R,T) gravity," *Can. J. Phys.*, vol. 98, pp. 109 (2020).

[20] M. Li, "A Model of Holographic Dark Energy," *Phys. Lett. B*, vol. 603, pp. 1 (2004).

[21] L. Susskind, "The World as a Hologram," *J. Math. Phys.*, vol. 36, pp. 6377 (1995).

[22] A. G. Cohen, D. B. Kaplan, and A. E. Nelson,, "Effective Field Theory, Black Holes, and the Cosmological Constant," *Phys. Rev. Lett.*, vol. 82, pp. 4971 (1999).

[23] Z. K. Guo, Y. S. Piao, X. Zhang, and Y. Z. Zhang, "Two-field quintom models in the w-ω plane," *Phys. Rev. D*, vol. 74, pp. 127304 (2006).

[24] L. N. Granda and A. Oliveros, "Infrared cut-off proposal for the Holographic density," *Phys. Lett. B*, vol. 669, pp. 275–279 (2008).

[25] H. Wei and R. G. Cai, "A New Model of Agegraphic Dark Energy," *Phys. Lett. B*, vol. 660, pp. 113–117 (2008).

[26] D. Pavon and W. Zimdahl, "Holographic dark energy and cosmic coincidence," *Class. Quantum Grav.*, vol. 24, pp. 5461–5470 (2007).

[27] S. Nojiri and S. D. Odintsov, "Unifying phantom inflation with late-time acceleration: scalar phantom-non-phantom transition model and generalized holographic dark energy," *Gen. Rel. Grav.*, vol. 38, pp. 1285–1304 (2006).

[28] S. Nojiri, S. D. Odintsov, and E. N. Saridakis, "Modified cosmology from extended entropy with varying exponent," *Eur. Phys. J. C*, vol. 79, pp. 242 (2019).

[29] S. Nojiri, S. D. Odintsov, and E. N. Saridakis, "Different faces of generalized holographic dark energy," *Symmetry*, vol. 13 no. 6, pp. 928 (2021).

[30] M. Tavayef, A. Sheykhi, K. Bamba, and H. Moradpour, "Tsallis holographic dark energy," *Phys. Lett. B*, vol. 781, pp. 195–200 (2018).

[31] C. Tsallis and L. J. L. Cirto, "Black hole thermodynamical entropy," *Eur. Phys. J. C*, vol. 73, pp. 2487 (2013).

[32] S. Nojiri, S. D. Odintsov, and E. N. Saridakis, "How fundamental is entropy? From non-extensive statistics and black hole physics to the holographic dark universe," arXiv:2201.02424 (2022).

[33] A. S. Jahromi, S. A. Moosavi, H. Moradpour, J. P. M. González, E. Sadri, and I. G. Salako, "Generalized entropy formalism and a new holographic dark energy model," *Phys. Lett. B*, vol. 780, pp. 21–24 (2018).

[34] A. Majhi, "Non-extensive statistical mechanics and black hole entropy from quantum geometry," *Phys. Lett. B*, vol. 775, pp. 32–36 (2017).

[35] H. Moradpour, S. A. Moosavi, I. G. Salako, A. Jawad, and S. Ghaffari, "Thermodynamic approach to holographic dark energy and the Rényi entropy," *Eur. Phys. J. C*, vol. 78, pp. 829 (2018).

[36] C. Tsallis, "Possible generalization of Boltzmann-Gibbs statistics," *J. Stat. Phys.*, vol. 52, pp. 479–487 (1988).

[37] M. Younas, S. Hanif, I. Hussain, and M. F. Malik, "Cosmological Implications of the Generalized Entropy Based Holographic Dark Energy Models in Dynamical Chern-Simons Modified Gravity," *Advances in High Energy Physics*, vol. 2019, pp. 1287932 (2019).

[38] S. Ghaffari, A. Sheykhi, and M. H. Dehghani, "Tsallis holographic dark energy in Fractal Universe," *Phys. Dark Univ.*, vol. 23, pp. 100246 (2019).

[39] Y. Aditya, U. Y. D. Prasanthi, "Observational constraint on interacting Tsallis holographic dark energy in logarithmic Brans-Dicke theory," *Eur. Phys. J. C*, vol. 79, pp. 1020 (2019).

[40] S. Maity and U. Debnath, "Tsallis, Rényi and Sharma-Mittal holographic and new agegraphic dark energy models in D-dimensional fractal universe," *Eur. Phys. J. Plus*, vol. 134, pp. 514 (2019).

[41] A. Iqbal and A. Jawad, "Tsallis, Renyi and Sharma–Mittal holographic dark energy models in DGP brane-world," *Phys. Dark Univ.*, vol. 26, pp. 100349 (2019).

[42] A. Jawad, A. Iqbal, and A. H. Bokhari, "Tsallis, Rényi and Sharma-Mittal Holographic Dark Energy Models in Loop Quantum Cosmology," *Symmetry*, vol. 10, pp. 635 (2018).

[43] Y. Aditya and U. Y. D. Prasanthi, "Dynamics of Sharma-Mittal holographic dark energy model in Brans-Dicke theory of gravity," *Bulgarian Astronomical Journal*, vol. 38, pp. 52–59 (2023).

[44] U. Y. D. Prasanthi and Y. Aditya, "Anisotropic Renyi holographic dark energy models in general relativity," *Results Phys.*, vol. 17, pp. 103101 (2020).

[45] U. Y. D. Prasanthi and Y. Aditya, "Observational constraints on Renyi holographic dark energy in Kantowski-Sachs universe," *Phys. Dark Univ.*, vol. 31, pp. 100782 (2021).

[46] Y. Aditya, S. Mandal, P.K.Sahoo, D. R. K. Reddy "Observational constraint on interacting Tsallis holographic dark energy in logarithmic Brans-Dicke theory," *Eur. Phys. J. C*, vol. 79, pp. 1020 (2019).

[47] Y. Aditya and D. R. K. Reddy, "Dynamics of perfect fluid cosmological model in the presence of massive scalar field in f(R,T) gravity," *Astrophys. Space Sci.*, vol. 364, pp. 3 (2019).

[48] Y. Aditya and D. R. K. Reddy, "FRW type Kaluza-Klein modified holographic Ricci dark energy models in Brans-Dicke theory of gravitation," *Eur. Phys. J. C*, vol. 78, pp. 619 (2018).

[49] Y. Aditya and D. R. K. Reddy, "Anisotropic new holographic dark energy model in Saez-Ballester theory of gravitation," *Astrophys. Space Sci.*, vol. 363, pp. 207 (2018).

[50] K. D. Naidu, D. C. Papa Rao, and D. R. K. Reddy, "Dynamics of axially symmetric anisotropic modified holographic Ricci dark energy model in Brans-Dicke theory of gravitation," *Eur. Phys. J. Plus*, vol. 133, pp. 303 (2018).

[51] M. V. Santhi, V. U. M. Rao, D. M. Gusu, and Y. Aditya., "Bianchi type-III holographic dark energy model with quintessence," *Int. J. Geom. Methods in Modern Phys.*, vol. 15, pp. 1850161 (2018).

[52] M.V. Santhi, V.U.M. Rao and Y. Aditya "Anisotropic Generalized Ghost Pilgrim Dark Energy Model in General Relativity," *Int. J. Theor. Phys.*, vol. 56, pp. 362 (2017).

[53] M. V. Santhi, V. U. M. Rao, Y. Aditya "Anisotropic magnetized holographic Ricci dark energy cosmological model," *Can. J. Phys.*, vol. 95, pp. 381-392 (2017).

[54] M. V. Santhi, V. U. M. Rao and Y. Aditya "Bianchi type-VI0 modified holographic Ricci dark energy model in a scalar–tensor theory," *Can. J. Phys.*, vol. 95, pp. 179 (2017).

[55] D. R. K. Reddy, S. Anitha, and S. Umadevi, "Anisotropic holographic dark energy model in Bianchi type-VI0 universe in a scalar-tensor theory of gravitation," *Astrophys. Space Sci.*, vol. 361, pp. 349 (2016).

[56] D. R. K. Reddy, S. Anitha, S. Umadevi "Five dimensional minimally interacting holographic dark energy model in Brans-Dicke theory of gravitation," *Astrophys. Space Sci.*, vol. 361, pp. 356 (2016).

[57] M. V. Santhi, Y. Aditya, V. U. M. Rao "Some Bianchi type generalized ghost pilgrim dark energy models in general relativity," *Astrophys. Space Sci.*, vol. 361, pp. 142 (2016).

[58] M. V. Santhi, V. U. M. Rao, Y. Aditya "LRS Bianchi type-V universe with variable modified Chaplygin gas in a scalar–tensor theory of gravitation," *Can. J. Phys.*, vol. 94, pp. 578 (2016).

[59] R. L. Naidu, Y. Aditya, D.R.K. Reddy "Bianchi type-V dark energy cosmological model in general relativity in the presence of massive scalar field," *Heliyon*, vol. 5, pp. 01645 (2019).

[60] D. R. K. Reddy, Y. Aditya, G. Ramesh "Dynamical anisotropic dark energy cosmological model in general relativity," *Journal of Dynamical Systems and Geometric Theories*, vol. 17, pp. 1 (2019).

[61] R. L. Naidu, "Bianchi type-II modified holographic Ricci dark energy cosmological model in the presence of massive scalar field," *Can. J. Phys.*, vol. 97, pp. 330 (2019).

[62] Y. Aditya, K. Deniel Raju, V. U. M. Rao, D. R. K. Reddy "Kaluza-Klein dark energy model in Lyra manifold in the presence of massive scalar field," *Astrophys. Space Sci.*, vol. 364, pp. 190 (2019).

[63] Y. Aditya and D. R. K. Reddy, "Dynamics of perfect fluid cosmological model in the presence of massive scalar field in f(R,T) gravity," *Astrophys. Space Sci.*, vol. 364, pp. 3 (2019).

[64] K. Deniel Raju, T. Vinutha, Y. Aditya, D.R.K. Reddy "Bianchi type-V string cosmological model with a massive scalar field," *Astrophys. Space Sci.*, vol. 365, pp. 28 (2020).

[65] K. Deniel Raju, Y. Aditya, V. U. M. Rao, D. R. K. Reddy "Bianchi type-III dark energy cosmological model with massive scalar meson field," *Astrophys. Space Sci.*, vol. 365, pp. 45 (2020).

[66] K. D. Raju, M. B. Rao, Y. Aditya, T. Vinutha, D. R. K. Reddy "Kantowski-Sachs universe with dark energy fluid and massive scalar field," *Can. J. Phys.*, vol. 97, pp. 932 (2019).

[67] Y. Aditya, K. D. Raju, pp. J. Ravindranath, “Dynamical aspects of anisotropic Bianchi type VI0 cosmological model with dark energy fluid and massive scalar field,” *Indian J. Phys.*, vol. 95, pp. 383–389 (2021).

[68] K. D. Naidu, Y. Aditya, R.L. Naidu, D.R.K. Reddy “Kaluza-Klein minimally interacting dark energy model in the presence of massive scalar field,” *Mod. Phys. A*, vol. 36, no. 8, pp. 2150054 (2021).

[69] R. L. Naidu, Y. Aditya, K. Deniel Raju, T. Vinutha, D. R. K. Reddy “Kaluza-Klein FRW dark energy models in Saez-Ballester theory of gravitation,” *New Astron.*, vol. 85, pp. 101564 (2021).

[70] M. pp. V. V. Bhaskara Rao, R. L. Naidu, Y. Aditya, D. R. K. Reddy “Bianchi type–I dark energy cosmological model coupled with a massive scalar field,” *New Astron.*, vol. 92, pp. 101733 (2022).

[71] M. pp. V. V. Bhaskara Rao, Y. Aditya, U. Y. Divya Prasanthi, D. R. K. Reddy “Anisotropic minimally interacting dark energy models with cosmic strings and a massive scalar field,” *Int. J. Mod. Phys. A*, vol. 36, no. 36, pp. 2150260 (2021).

[72] Y. Aditya, U. Y. Divya Prasanthi, D. R. K. Reddy “Bianchi type-IX model in the presence of anisotropic dark energy and massive scalar meson field in Lyra geometry,” *Int. J. Mod. Phys. A*, vol. 37, no. 16, pp. 2250107 (2022).

[73] Y. Aditya, “Anisotropic cosmological model with a massive scalar field in f(R,T) gravity,” *Bulgarian Astronomical Journal*, vol. 39 (2023).

[74] V. U. M. Rao, U. Y. Divya Prasanthi, Y. Aditya “Plane symmetric modified holographic Ricci dark energy model in Saez-Ballester theory of gravitation,” *Results Phys.*, vol. 10, pp. 469 (2018).

[75] Y. Aditya, R. L. Naidu, D. R. K. Reddy “Non-vacuum plane symmetric model in f(R) theory of gravity,” *Results Phys.*, vol. 12, pp. 339 (2019).

[76] Y. Aditya, U. Y. Divya Prasanthi, D. R. K. Reddy “Plane-symmetric dark energy model with a massive scalar field,” *New Astron.*, vol. 84, pp. 101504 (2021).

[77] K. S. Thorne, “Primordial Element Formation, Primordial Magnetic Fields, and the Isotropy of the Universe,” *Astrophys. J.*, vol. 148, pp. 51 (1967).

[78] R. Kantowski and R. K. Sachs, "Some Spatially Homogeneous Anisotropic Relativistic Cosmological Models," *Math Phys.*, vol. 7, pp. 433 (1966).

[79] J. Kristian and R. K. Sachs, "Observations in Cosmology," *Astrophys. J.*, vol. 143, pp. 379 (1966).

[80] C.B. Collins, E.N. Glass, and D. A. Wilkinson, "Exact spatially homogeneous cosmologies," *Gen. Relativ. Gravit.*, vol. 12, pp. 805 (1980).

[81] V. B. Johri and K. Desikan, "Cosmological models with constant deceleration parameter in Brans-Dicke theory," *Gen. Relativ. Gravit.*, vol. 26, pp. 1217 (1994).

[82] V. B. Johri and R. Sudharsan, "BD-FRW Cosmology with Bulk Viscosity," *Aust. J. Phys.*, vol. 42, pp. 215 (1989).

[83] A. Pradhan, M. K. Jasim, and pp. K. Sahoo, "Dark energy models with anisotropic fluid in Bianchi type-VI0 space-time with time dependent deceleration parameter," *Astrophys. Space Sci.*, vol. 337, pp. 401–413 (2012).

[84] R. K. Mishra, A. Pradhan, Ch. Chawla "Anisotropic viscous fluid cosmological models from deceleration to acceleration in string cosmology," *Int. J. Theor. Phys.*, vol. 52, pp. 2546–2559 (2013).

[85] V. U. M. Rao and U. Y. Divya Prasanthi, "Bianchi type-I and -III modified holographic Ricci dark energy models in Saez-Ballester theory," *Eur. Phys. J. Plus*, vol. 132, pp. 64 (2017).

[86] H. Amirhashchi, A. Pradhan, H. Zainuddin "An interacting and non-interacting two-fluid dark energy models in FRW universe with time dependent deceleration parameter," *Int. J. Theor. Phys.*, vol. 50, pp. 3529–3543 (2011).

[87] R. K. Mishra, A. Chand, A. Pradhan "Dark energy models in f(R, T) theory with variable deceleration parameter," *Int. J. Theor. Phys.*, vol. 55, pp. 1241–1256 (2016).

[88] A. Jawad, U. Debnath "Generalized ghost pilgrim scalar field models of dark energy," *Commun. Theor. Phys.*, vol. 64, pp. 590 (2015).

[89] J. V. Cunha, "Kinematic constraints to the transition redshift from supernovae type Ia union data," *Phys. Rev. D*, vol. 79, pp. 047301 (2009).

[90] Z. Li, pp. Wu, H. Yu "Examining the cosmic acceleration with the latest Union2 supernova data," *Phys. Lett. B*, vol. 695, pp. 1 (2011).

[91] H. Amirhashchi and S. Amirhashchi, "Current constraints on anisotropic and isotropic dark energy models," *Phys. Rev. D*, vol. 99, pp. 023516 (2019).

[92] S. Capozziello, Ruchika, Anjan A Sen"Model-independent constraints on dark energy evolution from low-redshift observations," *MNRAS*, vol. 484, pp. 4484 (2019).

[93] N. Aghanim, Y. Akrami, M. Ashdown, J. Aumont, C. Baccigalupi, M. Ballardini, A. J. Banday, R. B. Barreiro, N. Bartolo, S. Basak, R. Battye, K. Benabed, J.-P. Bernard, M. Bersanelli, pp. Bielewicz, J. J. Bock, J. R. Bond, J. Borrill, F. R. Bouchet, F. Boulanger, M. Bucher, C. Burigana, R. C. Butler, E. Calabrese, J.-F. Cardoso, J. Carron, A. Challinor, H. C. Chiang, J. Chluba, L. pp. L. Colombo, C. Combet, D. Contreras, B. pp. Crill, F. Cuttaia, pp. de Bernardis, G. de Zotti, J. Delabrouille, J.-M. Delouis, E. Di Valentino, J. M. Diego, O. Doré, M. Douspis, A. Ducout, X. Dupac, S. Dusini, G. Efstathiou, F. Elsner, T. A. Enßlin, H. K. Eriksen, Y. Fantaye, M. Farhang, J. Fergusson, R. Fernandez-Cobos, F. Finelli, F. Forastieri, M. Frailis, A. A. Fraisse, E. Franceschi, A. Frolov, S. Galeotta, S. Galli, K. Ganga, R. T. Génova-Santos, M. Gerbino, T. Ghosh, J. González-Nuevo, K. M. Górski, S. Gratton, A. Gruppuso, J. E. Gudmundsson, J. Hamann, W. Handley, F. K. Hansen, D. Herranz, S. R. Hildebrandt, E. Hivon, Z. Huang, A. H. Jaffe, W. C. Jones, A. Karakci, E. Keihänen, R. Keskitalo, K. Kiiveri, J. Kim, T. S. Kisner, L. Knox, N. Krachmalnicoff, M. Kunz, H. Kurki-Suonio, G. Lagache, J.-M. Lamarre, A. Lasenby, M. Lattanzi, C. R. Lawrence, M. Le Jeune, pp. Lemos, J. Lesgourgues, F. Levrier, A. Lewis , M. Liguori, pp. B. Lilje, M. Lilley, V. Lindholm, M. López-Caniego, pp. M. Lubin, Y.-Z. Ma, J. F. Macías-Pérez, G. Maggio, D. Maino, N. Mandolesi, A. Mangilli, A. Marcos-Caballero, M. Maris, pp. G. Martin, M. Martinelli, E. Martínez-González, S. Matarrese, N. Mauri, J. D. McEwen, pp. R. Meinhold, A. Melchiorri, A. Mennella, M. Migliaccio, M. Millea, S. Mitra, M.-A. Miville-Deschênes, D. Molinari, L. Montier, G. Morgante, A. Moss, pp. Natoli, H. U. Nørgaard-Nielsen, L. Pagano, D. Paoletti, B. Partridge, G. Patanchon, H. V. Peiris, F. Perrotta, V. Pettorino, F. Piacentini, L. Polastri, G. Polenta, J.-L. Puget, J. pp. Rachen, M. Reinecke, M. Remazeilles, A. Renzi, G. Rocha, C. Rosset, G. Roudier, J. A. Rubiño-Martín, B. Ruiz-Granados, L. Salvati, M. Sandri, M. Savelainen, D. Scott, E. pp. S. Shellard, C. Sirignano, G. Sirri, L. D. Spencer, R. Sunyaev, A.-S. Suur-Uski, J. A. Tauber, D. Tavagnacco, M. Tenti, L. Toffolatti, M. Tomasi, T. Trombetti, L. Valenziano, J. Valiviita,

B. Van Tent, L. Vibert, pp. Vielva, F. Villa, N. Vittorio, B. D. Wandelt, I. K. Wehus, M. White, S. D. M. White, A. Zacchei, A. Zonca "Planck 2018 results. VI. Cosmological parameters," *A&A*, vol. 641, pp. A6 (2018).

[94] R. R. Caldwell and E. V. Linder, "Limits of Quintessence," *Phys. Rev. Lett.*, vol. 95, pp. 141301 (2005).

[95] V. Sahni, T. D. Saini, A. A. Starobinsky, U. Alam "A new geometrical diagnostic of dark energy," *J. Exp. Theor. Phys. Lett.*, vol. 77, pp. 201 (2003).

[96] C. pp. Singh and pp. Kumar, "Statefinder diagnosis for holographic dark energy models in modified f(R, T) gravity," *Astrophys. Space Sci.*, vol. 361, pp. 157 (2016).

[97] S. Nojiri, S. D. Odintsov, E. M. Saridakis "Holographic inflation," *Phys. Lett. B*, vol. 797, pp. 134829 (2019).

[98] E. Elizalde and A. V. Timoshkin, "Viscous fluid holographic inflation," *Eur. Phys. J. C*, vol. 79, pp. 732 (2019).

[99] S. Nojiri, S. D. Odintsov, V. K. Oikonomou, T. Paul "Unifying Holographic Inflation with Holographic Dark Energy: a Covariant Approach," *Phys. Rev. D*, vol. 102, pp. 023540 (2020).

Received September, 2023